Thalamus & Related Systems, page 1 of 13. ©2007 Cambridge University Press
doi:10.1017/S1472928807000283 Printed in the United Kingdom

Reorganization of barrel circuits leads to thalamically-evoked cortical epileptiform activity

QIAN-QUAN SUN[1,2], JOHN R. HUGUENARD[1] AND DAVID A. PRINCE[1]

[1]Dept. Neurology and Neurological Sciences, Stanford Univ., Stanford, CA 94305, USA and [2]Dept. Zoology and Physiology, Univ. Wyoming, Laramie, WY 82072, USA

We have studied circuit activities in layer IV of rat somatosensory barrel cortex that contains microgyri induced by neonatal freeze lesions. Structural abnormalities in GABA-containing interneurons are present in the epileptogenic paramicrogyral area (PMG). We therefore tested the hypothesis that decreased postsynaptic inhibition within barrel microcircuits occurs in the PMG and contributes to epileptogenesis when thalamocortical afferents are activated. In thalamocortical (TC) slices from naïve animals, single electrical stimuli within the thalamic ventrobasal (VB) nucleus evoked transient cortical multi-unit activity lasting 65 ± 42 msec. Similar stimuli in TC slices from lesioned barrel cortex elicited prolonged (850 ± 100 msec) paroxysmal discharges that originated in the PMG and propagated laterally over several mm. The duration of paroxysmal discharges were shortened by ~70% when APV was applied and were abolished by CNQX. The cortical paroxysmal discharges did not evoke thalamic oscillations. Whole-cell patch-clamp recordings show that there is a shift in the balance of TC-evoked responses in the PMG that favors excitation over inhibition. Dual, whole-cell recordings in layer IV of the PMG indicated that selective loss of inhibition from fast-spiking interneurons to spiny neurons in the barrel circuits is likely to contribute to unconstrained cortical recurrent excitation with generation and spread of paroxysmal discharges.

Keywords: Thalamocortical slices, epileptogenesis, inhibition, interneurons, microgyri

INTRODUCTION

Integration and processing of sensory information carried by thalamocortical (TC) axons to the neocortex requires precisely timed activation of excitatory and inhibitory neurons (Sillito, 1977; Simons, 1978; Agmon and Connors, 1991; Agmon and Connors, 1992; Kim *et al.*, 1995; Porter *et al.*, 2001). Inhibitory interneurons have an important role in gating sensory input and shaping receptive fields (Sillito, 1977), as well as limiting recurrent excitation present among spiny neurons (Feldmeyer *et al.*, 1999; Sun *et al.*, 2006). A cohort of morphologically distinct excitatory cells and inhibitory interneurons has been described in layer IV barrels (Woolsey, 1967; Keller and White, 1987). Different subtypes of inhibitory neurons located in the barrel cortex also form inhibitory networks coupled by electrical and chemical synapses that have important functional roles (Gibson *et al.*, 1999; Beierlein *et al.*, 2000). Using paired intracellulular recordings we have previously studied the properties of synaptic connections between spiny neurons (i.e. spiny stellate and pyramidal cells) and interneurons, and the integration of TC input, in layer IV barrels of rat TC slices (Sun *et al.*, 2006). We found that whereas inhibition from regular-spiking non-pyramidal (RSNP) interneurons to spiny neurons is comparable in strength to excitatory connections, inhibition mediated by fast-spiking (FS) interneurons is ten times more powerful. TC excitatory postsynaptic potentials (EPSPs) elicit reliable, precisely timed action potentials in FS neurons, and a few FS neurons mediate TC feed-forward inhibition onto each spiny neuron. This inhibition can powerfully shunt TC-mediated excitation. The ready activation of FS cells by TC input, coupled with powerful, feed-forward inhibition would influence sensory processing profoundly *in vivo* and protect against runaway synaptic excitation, which occurs during epileptiform discharges (Sun *et al.*, 2006).

In the present experiments, we have examined the properties of neuronal responses to TC inputs in layer IV of rat barrel cortex in areas that are known to become epileptogenic after a developmental cortical injury. A focal, transcortical, freeze lesion at P1 in rats (Dvorak and Feit, 1977; Dvorak *et al.*, 1978; Jacobs *et al.*, 1996) results in development of a cortical microgyrus that is structurally similar to that which occurs in human epileptogenic polymicrogyria. Two anatomical alterations in the hyperexcitable cortex adjacent to the malformation, namely abnormal hyperinnervation by thalamocortical projections (Jacobs *et al.*, 1999c) and loss of parvalbumin-containing interneurons (Rosen *et al.*, 1998), is predicted to disrupt normal responses to TC inputs in layer IV of barrel cortex and contribute to epileptogenesis (reviewed in Jacobs *et al.*, 1999b). We tested this hypothesis in thalamocortical slices cut through microgyral sensory cortex.

At least 30 human syndromes result from disruption of the normal cortical developmental pattern (Schwartzkroin and Walsh, 2000). Human neocortical malformations are induced by both genetic and 'epigenetic' influences, including trauma and other insults to the immature brain that occur during either pregnancy or birth (Raymond *et al.*, 1995; Weinberger

Corresponding author:
J.R. HUGUENARD
Email: John.Huguenard@Stanford.Edu

and Lipska, 1995; Evrard, 1997; Evrard, 1988). Malformations resulting from aberrant patterns of brain development correlate with childhood seizure syndromes, as well as cognitive disabilities and other neurological disorders. A better understanding of the mechanisms underlying hyperexcitability in malformed cortex is potentially important for the development of novel therapeutic strategies. Several animal models have been studied that mimic various aspects of the histopathology and cortical hyperexcitability in human epileptogenic developmental malformations (Jacobs *et al.*, 1996; Lee *et al.*, 1997; Roper, 1998; Chevassus-Au-Louis *et al.*, 1999a; Chevassus-Au-Louis *et al.*, 1999b; Chevassus-Au-Louis and Represa, 1999; Jacobs *et al.*, 1999a; Jacobs *et al.*, 1999c). In the freeze lesion model of cortical microgyria (Dvorák and Feit, 1977; Dvorák *et al.*, 1978), cellular recordings and intracellular staining show that the region generating the epileptiform activity (the paramicrogyral zone or PMG) is not congruent with the microgyrus itself, but is adjacent to it (Jacobs *et al.*, 1999a). Although this adjacent region has normal gross cytoarchitecture, there are changes in synaptic strength and postsynaptic receptors (DeFazio and Hablitz, 1999; DeFazio and Hablitz, 2000; Hagemann *et al.*, 2003; Jacobs and Prince, 2005). Furthermore, there is evidence for structural reorganization including increased density of thalamocortical fibers and gross reorganization of cortical barrel structures in the PMG (Jacobs *et al.*, 1999c) and other abnormalities of afferent and efferent connectivity (Rosen *et al.*, 2000). There is also evidence for loss of parvalbumin-containing GABAergic interneurons within the PMG (Rosen *et al.*, 1998) as in irradiated rat models of cortical dysplasia and human dysplastic cortex (Roper *et al.*, 1997; Roper, 1998; Spreafico *et al.*, 1998; Alonso-Nanclares *et al.*, 2005; but see Schwarz *et al.*, 2000).

Although enhanced afferent and recurrent glutamatergic connections and/or loss of GABA-mediated inhibition might provide a sufficient substrate for generation of epileptiform activities, more detailed information is required to understand the role of maladaptive reorganization of local neocortical microcircuitry in epileptogenesis. One approach to this problem is to assess alterations in normal intracortical circuits activated by specific sensory inputs in areas of cortical malformations. In the present experiments, we took advantage of the preservation of thalamic projections to somatosensory cortex in rat thalamocortical slices (Agmon and Connors, 1991; Sasaki *et al.*, 2006; Inoue and Imoto, 2006) to study maladaptive synaptic connectivity and evoked paroxysmal activities in neocortical circuits of epileptogenic barrel cortex adjacent to freeze lesion-induced microgyri. Dual, whole-cell patch-clamp recordings in layer IV of the paramicrogyral cortex indicate that there is selective loss of inhibition from fast-spiking interneurons to spiny neurons in the barrel circuits that are likely to contribute to unconstrained cortical recurrent excitation and paroxysmal discharges.

METHODS

All experiments were performed in accordance with National Institutes of Health Guide for the Care and Use of Laboratory Animals and were approved by the Stanford University Institutional Animal Care and Use Committee. Freeze lesions were made as described previously (Jacobs *et al.*, 1996). Sprague-Dawley rat pups <48 hours old were immersed in ice for $\sim$4 min until movements and responses to tail pinch were absent. The skull was exposed through a scalp incision and a freezing probe with a circular tip (1 mm diameter) cooled to -50–-60°C was placed on the skull over somatosensory cortex $\sim$3 mm from the midline and 0.5 mm rostral to the bregma for 5–6 sec. The scalp was then sutured, the pup warmed and returned to the dam. This procedure routinely resulted in the development within barrel cortex of a microsulcus, consisting of an invagination of the cortical surface and an associated 4-layered microgyrus measuring $\sim$500 μm across. The microgyrus was clearly evident in fixed and live TC slices after P12 (Fig. 1) (Jacobs *et al.*, 1999c).

Brain slice preparation

After 13 $-$ 16 days, rats were anesthetized with pentobarbital (55 mg kg^{-1}, i.p.), decapitated, and brains removed and placed into cold ($\sim$4°C), oxygenated slicing medium containing (mM): 2.5 KCl, 1.25 NaH_2PO_4, 10.0 $MgCl_2$, 0.5 $CaCl_2$, 26.0 $NaHCO_3$, 11.0 glucose and 234.0 sucrose. The site of the previous freeze lesion was seen as a small depression in the pial surface that corresponded to the site of the microsulcus. The brains were removed quickly and TC slices (300 $-$ 400 μm) cut with a vibratome (TPI) in the above solution, according to methods of Agmon and colleagues (Agmon and Connors, 1991). Slices were transferred to a holding chamber where they were incubated (35°C) for $\geq$1 hour in artificial cerebrospinal fluid (ACSF) (below). Individual slices were then transferred to a recording chamber fixed to a modified microscope stage and allowed to equilibrate for $\geq$30 min before recording. Slices were submerged minimally and superfused continuously with oxygenated ACSF at 4.0 ml min^{-1}. The perfusion solution contained (mM): 126.0 NaCl, 2.5 KCl, 1.25 NaH_2PO_4, 1.0 $MgCl_2$, 2.0 $CaCl_2$, 26.0 $NaHCO_3$ and 10.0 glucose. Solutions were gassed with 95:5% O_2:CO_2 to a final pH of 7.4 at a temperature of 35 $\pm$ 1°C.

Silver staining was used to illustrate patterns of degenerating axonal fibers in the area in and around the microgyrus in some sections. Slices were fixed in 4% paraformaldehyde and 40-μm sections cut and mounted on gelatin coated slides. Sections were postfixed for 3 min in acid formalin, rinsed in glass distilled water and put in a solution of 15% silver nitrate, 10% potassium nitrate and 5% glycine for 15 min. Sections were then placed in a reducing solution of 1% pyrogallol, 1% nitric acid and 50% alcohol for 1 min, rinsed with glass-distilled water, fixed for 5 min in 5% sodium thiosulfate, dehydrated, cleared and mounted.

The barrel subfield and thalamus in TC slices were identified using a low-power objective (2.5$\times$) as described previously (Agmon and Connors, 1991). A water-immersion objective (40$\times$) with Nomarski optics and infrared video was used to visualize individual neurons in the barrel and either single or dual whole-cell patch-clamp recordings obtained. Recording pipettes were fabricated from capillary glass (World Precision Instruments, M1B150F-4) using a Sutter Instrument P80 puller, and had tip resistances of 2 $-$ 5 MΩ when filled with the intracellular solutions below. A Multiclamp 700 A amplifier (Axon Instruments) was used for voltage and current-clamp recordings from pairs of neurons. Biocytin (0.5%; Vector Labs) was added regularly to the patch-pipette solution for subsequent anatomical analysis. Patch-pipette saline was modified according to Brecht and Sakmann (Brecht and Sakmann, 2002) and was composed of

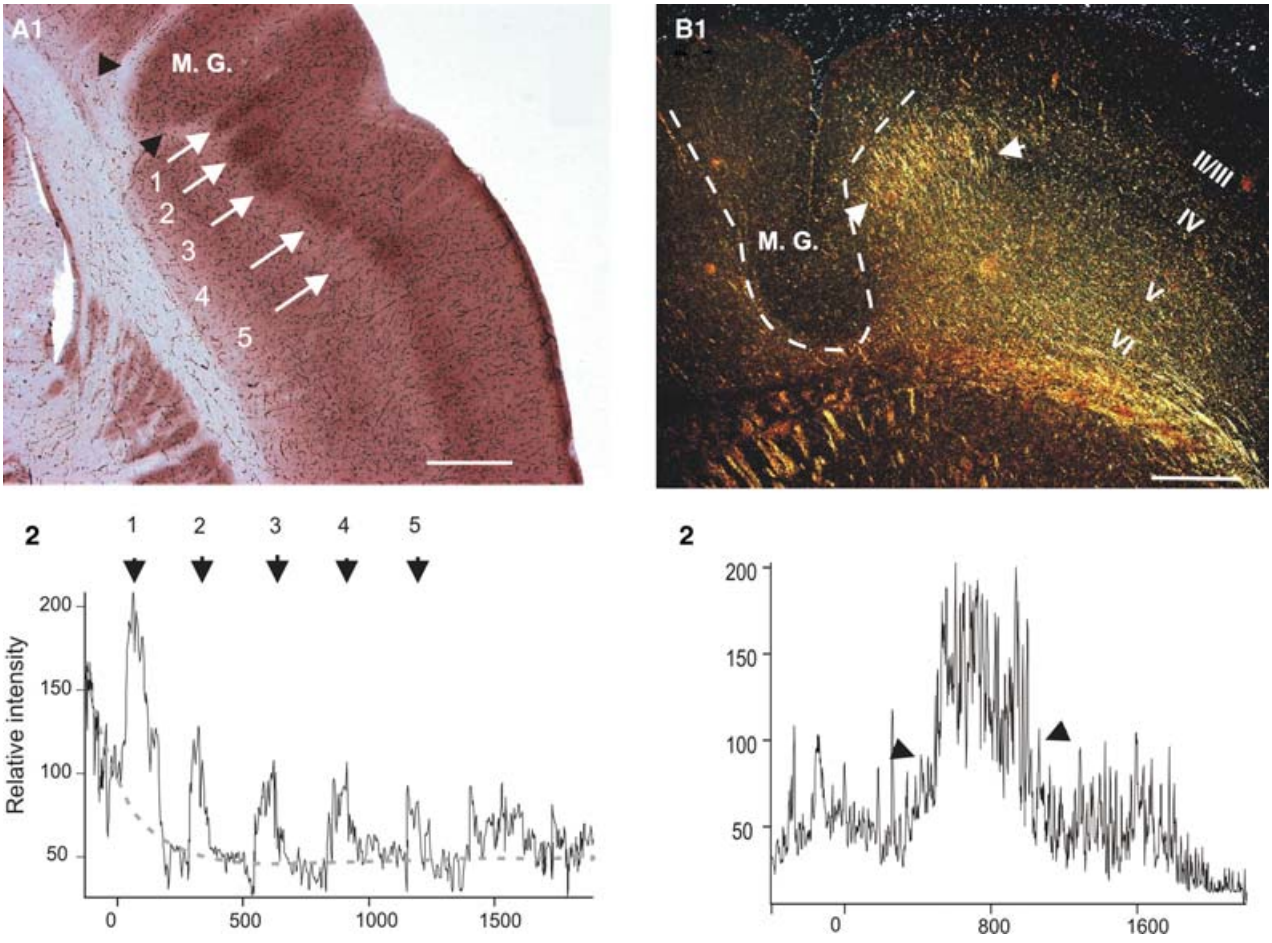

Fig. 1. Cytochrome C staining of layer IV barrels in rat somatosensory cortex containing a freeze lesion-induced microgyrus (M.G.). (A1) Photomicrograph of a fixed thalamocortical (TC) slice stained with cytochrome c. White arrows indicate barrels, which appear as darker areas in layer IV separated by lighter septa. (A2) Pixel intensities measured by a single pixel width line scan as a function of distance (μm) from the edge of the M.G. in the center of layer IV. Peaks in intensity identify barrels regions (arrows 1–5, as in A1) separated by the low-intensity septal regions. Note that the first barrel (1) in the PMG region has the most intense cytochrome c immunoreactivity. (B1) Darkfield micrograph of silver staining in TC section cut through layers I–VI of S–1 region of malformed neocortex (P40). Arrows indicate area of enhanced silver staining in layer IV adjacent to the M.G. II–VI indicate cortical lamina. (B2) Photographs were converted into grayscale images and analyzed as in A2. The brightness of pixels is quantified across the barrels in layer IV (x axis is distance in m from the edge of the M.G.). The area near the M.G. region had intense silver staining, whereas cortex within the M.G. showed little staining. Scale bars, 0.5 mm.

(mM): 100 K-gluconate, 10.0 phosphocreatine-Tris, 3.0 $MgCl_2$, 0.07 $CaCl_2$, 4 EGTA, 10.0 HEPES, 4.0 Na_2-ATP and 1.0 Na-GTP, pH adjusted to 7.4 and osmolarity adjusted to 280 mOsm·l^{-1}; $E_{Cl}- = -77$ mV. In several experiments, an intracellular solution containing 14 mM Cl^- was used to give an estimated E_{Cl} of ~ -55 mV (e.g. Figs 4 and 7). Data were accepted for analysis when access resistance in whole-cell recordings ranged from 4 to 12 MΩ, and was stable (<25% change) during the recording. Extracellular multiple-unit activities were recorded using monopolar tungsten electrodes (0.2–2 MΩ; Frederick Haer) and a Grass amplifier (bandwidth, 0.03–3 kHz). Current and voltage protocols were generated using PCLAMP8 software (Axon Instruments).

A sharpened bipolar tungsten electrode, placed in the internal capsule or VPM, was used to activate TC afferents. The approximate position of the stimulating electrode was within the TC projections, as estimated from the results of DiI applications reported by others (Agmon and Connors, 1991; Agmon *et al.*, 1995). In some slices, the stimulating electrode was repositioned closer to the internal capsule or striatum (CPu) to obtain an optimal TC response. Initially, the stimulus intensity was set at a subthreshold level and then increased gradually to evoke all-or-none EPSCs and increased further to obtain maximal amplitude responses. Monosynaptic EPSPs and excitatory postsynaptic currents (EPSCs) were evoked in fast-spiking (FS) interneurons and spiny neurons by TC stimuli. The term 'spiny neurons' is used throughout to refer to both spiny stellate and pyramidal cells (Sun *et al.*, 2006). Pyramidal cells and interneurons were identified visually during recordings (Sun *et al.*, 2006) and the cell type confirmed with biocytin labeling (below). In some experiments, TC slices were maintained in an interface chamber and recordings of cortical and thalamic evoked multiunit activity made with tungsten microelectrodes (Figs. 2 and 3).

Unitary PSP latency in paired recordings was defined as the time from the peak of the presynaptic AP to the peak of the postsynaptic PSP, whereas AP latency was the time from either the onset of an intracellular current pulse or an extracellular fiber stimulation to the peak of the evoked AP. Spontaneous IPSCs were recorded in spiny neurons as outward currents under voltage clamp at holding potentials more positive than −45 mV (Fig. 4) whereas sEPSCs were recorded as inward currents at E_{Cl}: ~ -77 mV. Cross-correlations were calculated with Clampfit 8.0.

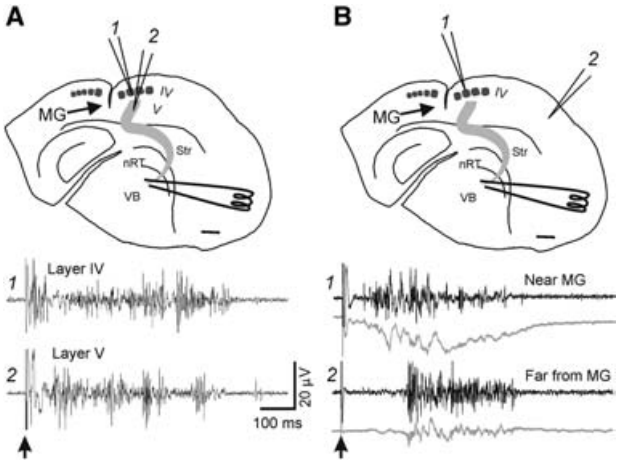

Fig. 2. Single electrical stimuli applied to the thalamic VB complex evoke epileptiform activities in the somatosensory cortical slices of FL-treated rats. (A) Top: Camera lucida reconstruction of TC slice from a FL rat. A microgyrus (MG, black arrow) was present in the face representation of barrel cortex. Barrels (gray regions in A and B) were visualized with bright-field microscopy in live slices and in fixed slices stained with cytochrome c. Dual simultaneous recordings of multiunit extracellular epileptiform activities in paramicrogyral layer IV (A1) and layer V (A2), evoked by single electrical stimuli (10 V, 5 μS, black arrow) applied to VB. In this and in Fig. 3, TC projection is shown in light gray. The evoked epileptiform activities in layers IV and V are similar in latency and duration at the two recording sites in the diagram. (B) Top: Electrodes were repositioned in the same slice as shown. Multi-unit extracellular activities, evoked with the same stimuli as in A1 and A2, recorded in layer IV at sites close to (B1) and at a distance (B2) from the border of the microgyrus. The epileptiform multi-unit activities (black) and field potentials (gray) had a shorter latency and longer duration at site 1 than site 2. Calibration in A2 applies to all measurements. Abbreviations: nRT, thalamic reticular nucleus; VB, thalamic ventrobasal complex; Str, striatum. IV, layer IV. Scale bars, 0.5 mm.

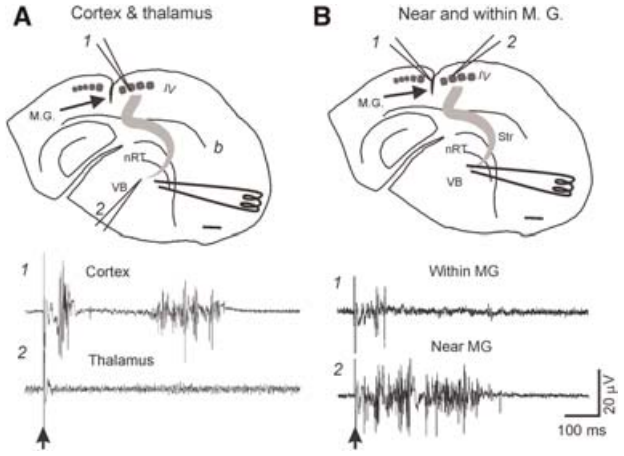

Fig. 3. Lack of thalamic and microgyral involvement in VB-evoked epileptiform responses in TC slices of FL treated rats. (A,B) Top: diagrams of slices as in Fig.2 showing locations of the microgyrus, barrels, and stimulating and recording electrodes. (A) The thalamic stimulus evoked an epileptiform event at long latency in layer IV of the paramicrogyral zone (site 1) but not in simultaneous recording from the relay nucleus (site 2). (B) Thalamic stimuli evoked long-duration, multiunit, epileptiform activities in layer IV of paramicrogyral cortex (site 2) but not within the microgyrus itself (site 1). Scale bars, 0.5 mm.

After recording, brain slices were fixed in 100 mM phosphate-buffered (PB) solution, pH 7.4, containing 1% paraformaldehyde and 2.5% glutaraldehyde at 4°C for ≥24 hours. Endogenous peroxidase was blocked by incubation in 1% H_2O_2 for 15 − 20 min. After several rinses in PB solution, slices were transferred to 1% avidin-biotinylated horseradish peroxidase complex containing 0.1% Triton X-100 in PB solution (ABC-Elite Camon) and left overnight at 4°C while being shaken lightly. The next day, slices were reacted using 3,3-diaminobenzidine (DAB; Sigma) and 0.01% H_2O_2 until dendrites and axonal arbors were clearly visible (∼2 − 5 min). Slices were mounted on glass slides, embedded in DPX-mounting media (Aldrich), and coverslipped.

Cytochrome oxidase staining (Wong-Riley, 1979) was used to identify the barrel structures in layer IV. Brain slices were stored overnight in 4% paraformaldehyde at 4°C. After several rinses in PB solution, they were resectioned at 100 μm and sections incubated in PB solution containing 50 mg DAB, 15 − 30 mg cytochrome c and 20 mg catalase/100 ml at 37°C for 2 hours in the dark. The reaction was stopped when individual barrels were clearly distinguishable from the background. After several rinses in PB solution, sections were mounted on glass slides, air-dried, defatted in absolute alcohol and xylene, embedded in DPX-mounting media (Aldrich) and coverslipped. Photomicrographs were converted into grayscale images and imported into IgorPro (Wavemetrics) for quantitative analysis.

Neuronal, three-dimensional reconstruction and morphometric measurements of dendritic and axonal arbors were

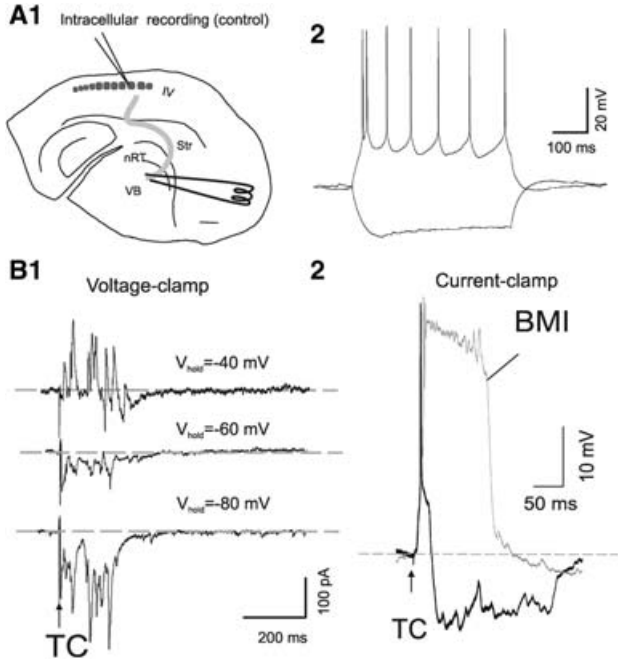

Fig. 4. Characterization of thalamically evoked synaptic activities in control layer IV neurons from unlesioned rat. (A1) Diagram as in Figs 2 and 3. (A2) Whole-cell current-clamp recording from a spiny neuron in a layer IV barrel, showing typical responses to 100 pA depolarizing and hyperpolarizing current pulses. (B1) Voltage-clamp recording (V_{hold} = −40, −60 and −80 mV) from the cell in A2. Single thalamic stimuli (TC, arrow) evoke a short latency, presumed monosynaptic EPSC followed by disynaptic and polysynaptic excitatory (inward, below dashed line) and inhibitory synaptic currents (outward, above dashed line.). E_{Cl} = −55 mV. (B2) Current-clamp recording from the neuron in (A) showing suprathreshold, thalamically evoked, depolarizing response followed by polysynaptic, hyperpolarizing IPSPs (black trace). Dashed line is pre-stimulus V_m. Bath application of bicuculline methiodide (BMI, 10 μM), eliminated the hyperpolarizing responses and led to the development of a prolonged, large amplitude depolarizing response (gray trace).

made with Neurolucida software (MicroBrightField). Cells and their processes were drawn with a camera lucida using 40× and 100× objectives. Biocytin histochemistry often resulted in background staining that allowed delineation of cortical laminae and barrel borders. In some slices, cytochrome oxidase histochemistry and labeling of single biocytin-filled neurons were combined to reveal the dendritic and axonal organization with respect to the barrel structure.

RESULTS

Histological sections showed that freeze lesion-induced microgyri, consisting of areas of abnormal lamination, were present within the barrel field (Fig. 1A1 M.G.) (Jacobs *et al.*, 1999c). The location of the microgyrus with respect to the barrel field is seen in live images of TC slices (not shown), which allows electrophysiological recordings from identified sites. After recording, slices were recovered and cytochrome c (CO) and Nissl stains used to establish the precise location of microgyri within in the barrel cortex. The widths of microgyri varied from 0.1 − 0.6 mm (e.g. Fig. 1A1). In 6 − 9 TC slices, enhanced CO staining was detected at the border between the 'normal' six-layered cortex and the three-layered microgyrus (e.g. Fig. 11A), which indicates that increased activity might occur in this region (Jacobs *et al.*, 1999a; Jacobs *et al.*, 1999c). In addition, consistent with previous results showing increased density of afferents and abnormal barrel structures (Jacobs *et al.*, 1999c), TC sections through the region of malformed neocortex showed enhanced silver stain in layer IV adjacent to the microgyrus (PMG) region in 6 − 9 slices from three animals (e.g. Fig. 1B).

Single thalamic stimuli elicit robust paroxysmal discharges in the FL cortex

We next examined the electrophysiological responses evoked by thalamic stimuli *in vitro*. Multiunit neocortical and thalamic activities were recorded in an interface chamber with tungsten microelectrodes from various locations in the neocortex (S1 and adjacent region) and thalamic relay nuclei. In naïve, untreated TC slices, single electrical stimuli applied to VB evoked transient cortical multi-unit activity lasting 65 ± 42 msec (not shown; $n = 6$). In the FL cortex, single stimuli elicited robust, prolonged, paroxysmal discharges with a duration of 850 ± 100 msec (Fig. 2) ($n = 6$). The duration of these epileptiform responses was shorter in minimally submerged slices used for voltage clamp recordings (Figs 2 and 7). Dual extracellular recordings showed that the epileptiform discharges were highly synchronous when electrodes were separated by <0.5 mm. The most intense paroxysmal activities were always recorded from the PMG, close to the border of the microgyrus ($n = 6$ slices from three rats) (Figs 2 and 3B). However, within the microgyri evoked activities were brief and less intense (mean durations 45 ± 15 msec, $n = 6$ slices from three rats) (Fig. 3B1). When one recording electrode was positioned laterally at various distances from the center of the lesion (i.e. the microsulcus), abnormal TC evoked activities were recorded for up to ~5 mm. The epileptiform discharges propagated laterally with a latency of ~100 msec at a distance of ~5 mm (mean propagation speed in layer IV, 50 ± 9 mm sec^{-1}, $n = 6$) (Fig. 2B). Paired simultaneous recordings in different laminae (excluding layer I) at the same distance from the microsulcus showed that the abnormal evoked activities were present and had a similar duration in layers II − VI (traces 1 and 2 in Fig. 2A). The paroxysmal discharges were reduced in duration by 70 ± 10% in APV (50 μM) and abolished by CNQX (10 μM), which indicates that the abnormal activities are mediated via activation of NMDA and AMPA receptors. Simultaneous thalamic and cortical recordings demonstrate that neocortical paroxysmal activity evoked by thalamic stimuli did not recruit thalamic oscillations (five out of five slices) (Fig. 3A), which indicates that the aberrant, prolonged neocortical discharge arises through recruitment of intracortical rather than thalamocortical circuits.

A shift in excitatory/inhibitory balance in the PMG

Layer IV neurons in the barrel cortex are the major targets for thalamic afferents (Woolsey and Van der Loos, 1970; Simons, 1978; Simons and Woolsey, 1979; Agmon and Connors, 1991). Anatomical results show that barrel structures in this lamina form abnormally (Jacobs *et al.*, 1999c), and extracellular recordings indicate that epileptiform activities are generated in layer IV (Figs 2 and 3). Therefore, we examined the mechanisms underlying the TC evoked paroxysmal activities by obtaining whole-cell patch-clamp recordings from neurons in layer IV of barrel cortex. In spiny cells of control slices ($n = 30$ cells), supramaximal extracellular TC stimuli evoked monosynaptic EPSCs followed by multi-peaked polysynaptic responses composed of mixed excitatory and inhibitory components (Fig. 4B). Initially, we used conditions that maximized detection of both excitatory and inhibitory ($GABA_A$ receptor-mediated) signals. Thus, the intracellular pipette solution contained a slightly elevated Cl^- concentration (14 mM, estimated $E_{Cl} \approx E_{GABA\text{-}A}$; −55 mV), and the voltage clamp holding potential was set positive to this (−40 mV trace of Fig. 4B1). Under these conditions, long-latency (150 ± 45 msec, $n = 10$ cells), presumed polysynaptic IPSCs were recorded as outward currents interspersed with polyphasic excitatory inward responses. At a V_{hold} of either −60 mV or −80 mV, the inhibitory responses became inward, and thalamically-evoked polysynaptic responses consisted of polyphasic inward currents likely composed of mixed EPSCs and IPSCs (Fig. 4B1). In current-clamp recordings, using patch pipettes containing physiological [Cl^-] (7 mM, estimated $E_{Cl} \approx E_{GABA\text{-}A}$: −77 mV), the TC stimulus evoked a single spike followed by a long-lasting (>100 msec) hyperpolarizing inhibitory response (8 ± 3 mV, $n = 10$ cells) (Fig. 4B2, control trace). To determine the role of inhibitory signaling in regulating the TC-evoked response, we applied the $GABA_A$ receptor antagonist bicuculline (10 μM), which resulted in the equivalent TC stimulus evoking an EPSP that triggered a spike followed by barrage of depolarizing PSPs and spikes resembling a paroxysmal depolarization shift (Fig. 4B2, BMI trace) (Matsumoto and Ajmone-Marsan, 1964; Prince, 1968). These results indicate that, in the normal barrel cortex *in vitro*, synchronous TC inputs evoke complex local cortical network activities that are composed predominantly of inhibitory responses that limit concurrent excitation (Sun *et al.*, 2006).

In FL-containing slices, supramaximal TC stimuli evoked multi-peaked, polysynaptic responses. In voltage-clamp recordings from neurons located far from the PMG region, the TC-evoked responses contained both inhibitory and excitatory synaptic events (Fig. 5A3,B). In cells in the PMG region, the same stimuli evoked predominantly inward currents (Fig. 5A2,B). Dual intracellular recordings of nearby cells in either region showed that the evoked activities were similar in duration and amplitude, indicating that the polysynaptic currents are probably generated by local network activities. To access the contributions of inward and outward currents to the overall polysynaptic local network activities, we compared the total charge of the PSCs at different distances from the edge of the microgyrus. In neurons close to the border of the microgyrus (0.3 mm), the overall charge of evoked polysynaptic events was positive (Fig. 5B), whereas the there was a progressive shift in the negative direction for neurons closer to the PMG (0.6 and 0.9 mm) (Fig 5B). These results indicate that in the epileptogenic PMG zone, the balance between excitation and inhibition in the local network shifts toward enhanced excitatory activities. The generation of paroxysmal network activities might result from either enhanced recurrent excitatory or reduced inhibitory synaptic connections.

To determine the strength of excitatory and inhibitory synaptic events in the epileptogenic PMG region, we obtained simultaneous whole-cell recordings from 30 pairs of cells in layer IV barrels near the PMG, of which nine pairs were connected synaptically. Interneurons and excitatory neurons were distinguished according to (1) their dendritic structures (either spiny or aspiny), (2) firing properties during current injections (McCormick *et al.*, 1985; Gupta *et al.*, 2000; Wang *et al.*, 2002) and (3) the GABAergic or glutamatergic nature of the unitary synaptic connection made by the neuron, which was verified routinely by estimating the reversal potential of the synaptic response and/or demonstrating sensitivity to CNQX (10 μM) and gabazine (10 μM). Unitary synaptic events were examined initially under current clamp by repeatedly eliciting short trains of action potentials (APs) alternately in presumed presynaptic and postsynaptic neurons (Fig. 6B1). Synaptic connections were confirmed by evoking >100 single action potentials at 1 Hz with brief depolarizing current pulses in presynaptic neurons. Both unitary excitatory postsynaptic potentials

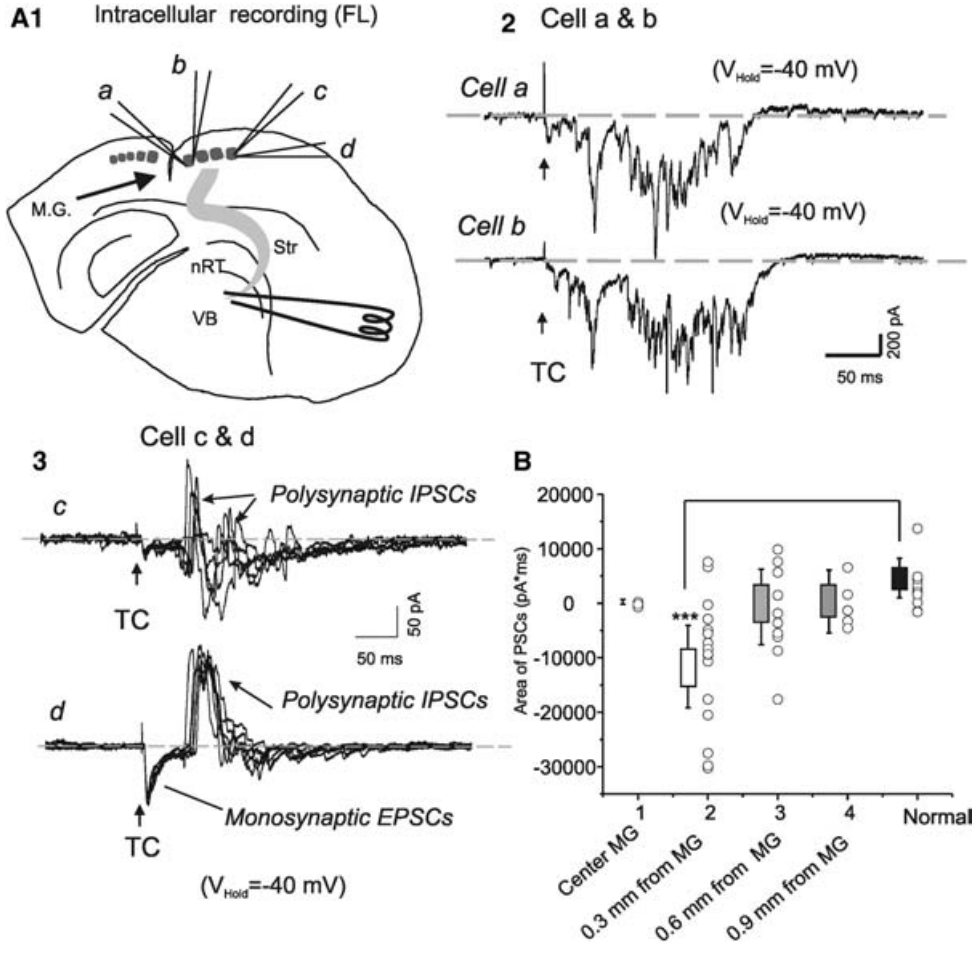

Fig. 5. Thalamically evoked synaptic activities in layer IV neurons located at different distances from the microgyrus. (A1) Diagram of slice and sites of recording. Simultaneous intracellular recordings were made from pairs of layer IV spiny neurons, each pair in a different barrel, as shown. (A2) Single thalamic stimuli (arrows) evoked monosynaptic EPSCs followed predominantly by polysynaptic excitatory (inward) currents in cells a and b. (A3) The same thalamic stimulus evoked monosynaptic EPSCs followed by inward and outward polysynaptic events in cells c and d. (B) Box/whisker and scatter plots (open circles) of total synaptic charge of the thalamically evoked polysynaptic events in all recorded layer IV neurons in areas 1 (within MG, 120 ± 540 pA ms^{-1}); 2 (0.2 – 0.4 mm from margin of MG, $13{,}500 \pm 7570$ pA ms^{-1}); 3 (0.6 mm from MG, 490 ± 6890 pA ms^{-1}), and 4 (0.9 mm from MG, 520 ± 5740 pA ms^{-1}) in TC slices from FL rats (see Fig. 1A). Normal, responses in layer IV neurons of naive rats (4700 ± 3650 pA ms^{-1}). $^{***}P < 0.001$.

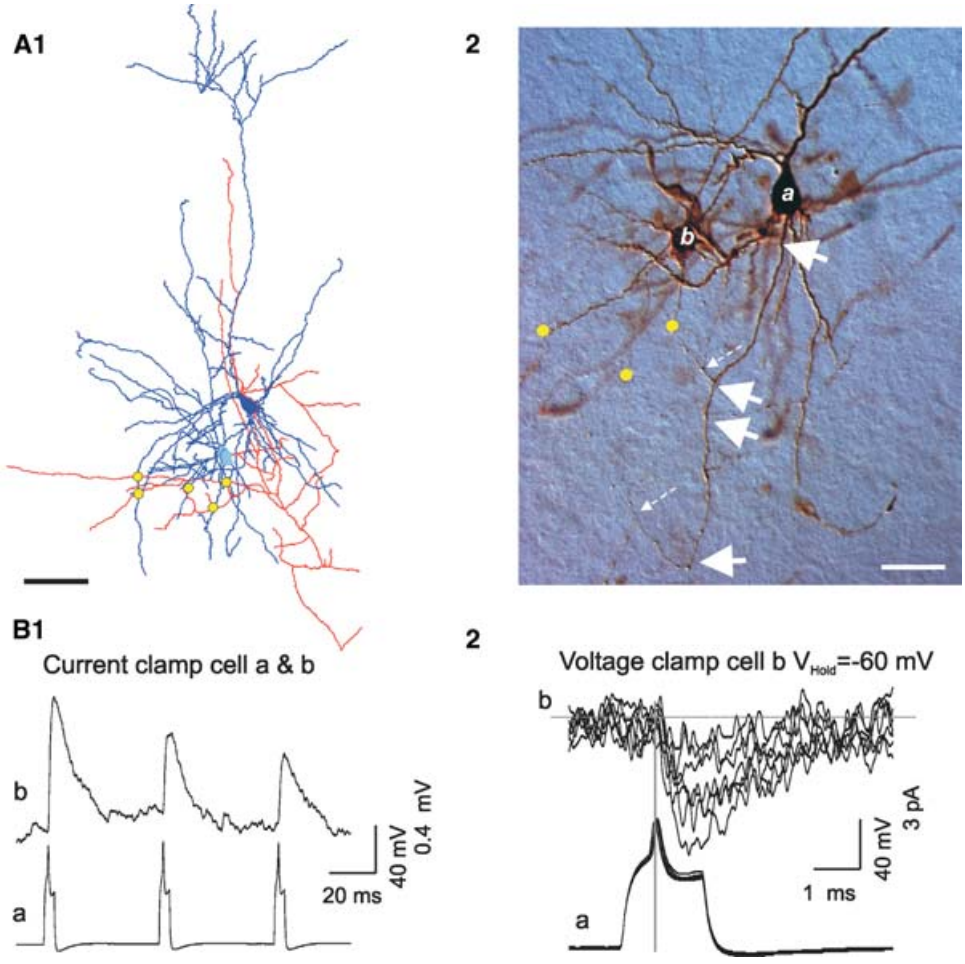

Fig. 6. Unitary excitatory responses in PMG cortex. (A1) Camera lucida reconstruction of a synaptically connected pair in layer IV, consisting of a star pyramidal neuron (cell body in blue, cell a in A2) and a spiny stellate cell (cell body in cyan, cell b in A2). Dendrites are in blue and axons in red. Scale bar, 100 μm. Yellow dots indicate sites of putative contact between axons of presynaptic cell (blue soma) and dendrites of postsynaptic cell (cyan soma) as identified from 100 microscopic images. (A2) Photomicrograph of the same cell pair (rotated slightly clockwise compared to A1). Note that the main axon (large arrows), which originates from the axon hillock of cell a, forms several collaterals along its path into deeper cortical layers. One of the branches (dashed small arrow) forms putative contacts on the dendrites of cell b. Another recurrent branch projects into layer IV and also forms putative contacts with cell b (close appositions are not visible in this focal plane). Scale bar, 50 μm. (B1) Current-clamp recording in both cells. Presynaptic APs in cell a (bottom trace, average of 20 trials) evoke uEPSPs in cell b. (B2) APs in cell a evoke fixed latency, variable amplitude uEPSCs in voltage-clamped cell b (6 traces overlaid). Vertical line, peak of APs in cell a.

(uEPSPs) (Fig. 6) and uIPSPs (Fig. 7) had short, fixed latencies (Figs 6B2 and 7B). In four of the nine synaptically connected pairs within PMG sites, presynaptic cells were spiny neurons and unitary EPSCs were recorded from the postsynaptic cell (Fig. 6B). In five pairs, presynaptic cells were FS interneurons and postsynaptic uIPSCs were evoked (Fig. 7B). Additional data from excitatory (11) and inhibitory (six) pairs recorded in layer IV of naïve, untreated brains have been published previously (Sun *et al.*, 2006) and are included as a control group in this study for comparison (Table 1). The recording conditions and ages of naïve animals and those with microgyri induced by freeze lesions were similar, and data obtained by the same investigator (Q-Q Sun).

Functional excitatory connections between adjacent layer IV neurons are not upregulated in the epileptogenic PMG region

Each pair of synaptically coupled neurons in the PMG. was within the same barrel, and there were no significant differences in amplitude, τ_{rise} and τ_{decay} for uEPSPs between excitatory neuronal pairs in naïve TC slices versus those in the PMG region of FL slices (Fig. 8). Analysis of recovered, biocytin-filled pairs of neurons with a 100× objective (Fig. 6A) demonstrated that the number of putative connections ($n = 4 \pm 2$ for four pairs of spiny cells in PMG and $n = 4 \pm 1$ for 11 spiny cell pairs in naïve brain slices) and the location of the connections (i.e. distance from the cell body) were similar in PMG and naïve slices.

Intracortical inhibition from basket cells is downregulated selectively in the epileptogenic PMG region

Unitary IPSPs between layer IV inhibitory and excitatory neurons were examined in five FS-excitatory pairs from naïve slices and five pairs in the PMG region of microgyrus-containing slices. In four of five pairs in the PMG, the postsynaptic excitatory neuron was a spiny stellate cell and in one it was a star pyramidal neuron. All

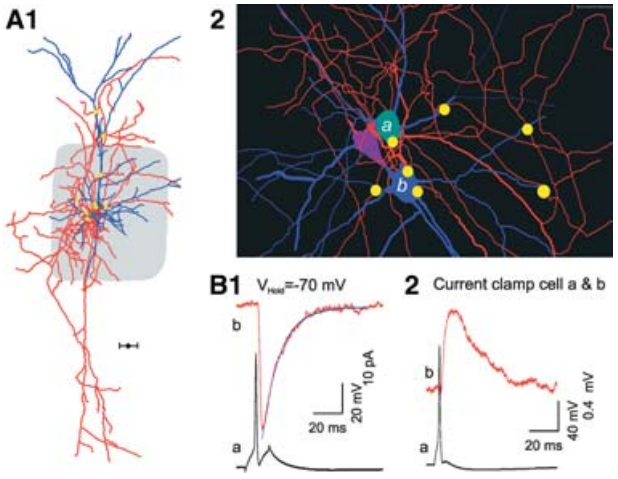

Fig. 7. Unitary inhibitory responses mediated by a fast-spiking basket cell in PMG cortex. (A1) Camera lucida reconstruction of a synaptically connected fast-spiking basket cell (green cell body) – spiny stellate neuron (red cell body) pair. Blue, dendrites; red, axons; gray shading, barrel structure. Scale bar, 20 μm. Yellow dots indicate putative contacts between axons of presynaptic fast-spiking cell and dendrites of postsynaptic spiny stellate cell identified from 100 microscopic images. (A2) Enlarged view of A1 (rotated clockwise ~160°) showing putative synaptic contacts from cell a onto the soma and dendrites of cell b. Close appositions are not seen between fast-spiking cell a and another adjacent spiny neuron (cell body in purple). (B1,B2) Unitary synaptic currents (B1) and potentials (B2) elicited in cell b by single APs in the presynaptic FS cell (a, black trace). AP in FS cell a (bottom trace) evokes a depolarizing uIPSC in spiny stellate cell (top trace). $E_{Cl} = -55$ mV.

postsynaptic neurons in the naïve cortex were star pyramidal cells. The properties of uIPSPs in the PMG cells were different from those in spiny cells of naïve slices in that the mean conductance was less than half of control values (Fig. 8B1, $P < 0.05$). However, there were no significant differences in either rise time (τ_{rise}) or decay time (τ_{decay}) for uIPSPs in control cortex versus PMG (Fig. 8B2-4).

The balance between inhibitory and excitatory synaptic strength shifts towards excitation in the epileptogenic PMG region

Reduced inhibition from FS to stellate cells alone should increase network excitability, but the ratio of unitary EPSC:IPSC strengths is also an important factor in determining whether afferent inputs recruit polysynaptic circuits. In naïve, untreated slices, the amplitude of uIPSPs received by layer IV stellate cells is $\sim 4-5\times$ larger than that of uEPSPs (5.0 ± 0.7 mV for uIPSPs and 1.1 ± 0.4 mV for uEPSPs, $P < 0.05$) and the decay time constant (τ_{decay}) $\sim 4\times$ longer for uIPSPs than for uEPSPs ($P < 0.05$). Thus, within this layer inhibition from FS to stellate cells is relatively stronger than the recurrent excitation between stellate cells. In the PMG region of FL-treated slices, peak conductance of uIPSCs was reduced dramatically (Fig. 8B) and approaches that of uEPSCs, which were not affected (Fig. 8A).

These results confirm our previous observations (Sun, *et al.*, 2006) that, in naïve slices, inhibition from single FS interneurons onto excitatory cells is far stronger than the unitary excitation that FS interneurons receive from single local excitatory neurons. The strength of inhibition from FS cells onto spiny neurons is decreased significantly in the PMG. This downregulation might be caused, in part, by a reduction in the number of putative inhibitory synaptic contacts per pair, because the number of close appositions between FS cell axons and spiny cells in pairs of labeled neurons appears to be less than in controls. In our earlier study (Sun *et al.*, 2006), basket cells in layer 4 formed $\sim 30 \pm 5$ putative contacts per spiny cell. In the four labeled pairs from the PMG, the average number of close appositions formed by the axon of a single FS cell onto a spiny neuron was $\sim 10 \pm 3$ (e.g. Fig. 7A2). However there were insufficient numbers of labeled pairs in the PMG to establish that this trend was significant.

Spontaneous excitatory and inhibitory synaptic events

We measured the properties of spontaneous IPSCs (sIPSCs) and sEPSCs to determine whether the specific deficits in FS to stellate cell inhibition in the PMG correlate with overall changes in synaptic input. Spontaneous synaptic events were recorded under voltage-clamp with pipette solution containing physiologically relevant [Cl^-] (7 mM, estimated $E_{Cl}-$: -77 mV) at different holding potentials (see Methods). In spiny neurons in the PMG, where we observed a reduction in uIPSC strength (Fig. 8), the amplitude of sIPSCs increased unexpectedly in both distal and proximal PMG zones (Table 1, areas 1 and 2). In addition, sIPSC frequency increased significantly, especially in the proximal PMG (Table 1, FL area 1,). By contrast, in cells within the microgyrus, the amplitude of sISPCs was smaller than controls and the frequency was unaffected (Table 1, FL area 0). Spontaneous EPSCs were largely unaffected, although there was a significant increase in their frequency in the proximal PMG (Table 2, FL area 1), the same location in which sIPSC frequency was elevated, indicating a general increase in connectivity within this zone.

DISCUSSION

We examined possible mechanisms that underlie epileptogenesis in rat barrel cortex subjected to a neonatal freeze lesion that produced a microgyral developmental malformation. The cell type, neuronal intrinsic properties and synaptic connections in barrel cortex are well characterized (Feldmeyer *et al.*, 1999; Feldmeyer *et al.*, 2002), making this a useful model in which to examine the relationship between epileptogenesis and structural reorganization (Jacobs *et al.*, 1999c; Rosen *et al.*, 2000), and alterations in GABAergic inhibitory circuitry (Rosen *et al.*, 1998; Jacobs and Prince, 2005) that are known to be present. Our results identify reductions in inhibitory synaptic strength as a major factor underlying hyperexcitability in barrel cortex adjacent to experimental microgyri.

The principal finding in these experiments is a reduction in inhibition from FS interneurons onto spiny cells in the area adjacent to the microgyrus. Known alterations in microgyral cortex might affect the strength of postsynaptic inhibition, including a transient reduction in the number of interneurons expressing parvalbumin (PV; presumed FS cells) that is present within the microgyrus and adjacent cortex until ~P21, and a decrease in the density of PV-containing cells in the PMG that persists into adulthood (Rosen *et al.*, 1998).

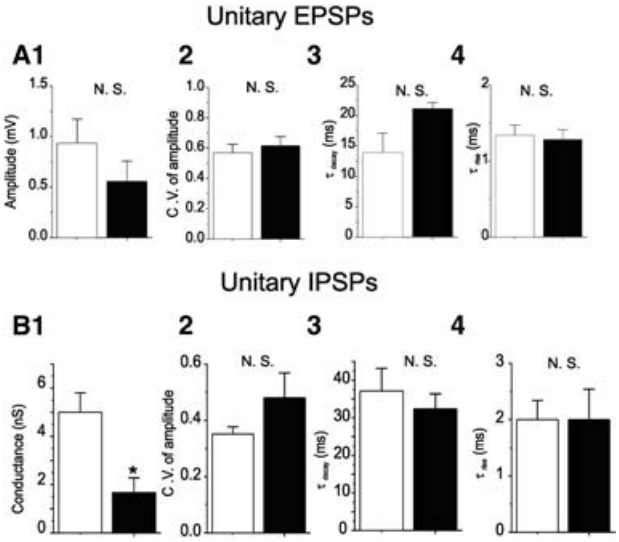

Fig. 8. Comparison of properties of uIPSCs and uEPSCs in normal and FL cortices. (A) Mean ± s.e.m. of uEPSPs recorded in layer IV of nave brains (open bars) and PMG of FL cortices (black bars). (A1) Amplitudes of uEPSPs recorded in current-clamp mode (Vm, −55 mV). (A2) Coefficient of variation (C.V.) of the amplitudes of uEPSPs. (A3) Decay time constant (τ) measured from single exponential decay for the uEPSPs. (A4) Rise time constant (τ) measured from single exponential equation for the uEPSPs. N.S., no statistical significance; $n = 11$ pairs for controls and $n = 4$ pairs for PMG. (B) Mean s.e.m. of uIPSCs recorded in layer IV of nave brain and PMG of FL cortices. V_m, −40 mV; E_{Cl}, −55 mV. (B1) Conductance of uIPSCs recorded in voltage-clamp mode. (B2) C.V. of the amplitudes of uIPSCs. (B3) Decay time constant (τ) measured from single exponential decay for the uEPSCs. (B4) Rise time constant (τ) measured from single exponential equation for the uEPSCs. $n = 11$ pairs for controls and $n = 5$ pairs for PMG.

Changes in $GABA_A$ receptors (Zilles *et al.*, 1998) are inferred from altered responses to GABAergic agonists (DeFazio and Hablitz, 1999). Depletion of FS interneurons should not affect the amplitude of uIPSCs in the current experiments if the remaining FS cells show similar connectivity. Notably, our recordings were obtained at P13 − 16 at a time when presumed FS cells still have reduced PV expression (Rosen *et al.*, 1998). This might indicate that structural and functional maturation of these cells is delayed, which might affect their ability to release GABA or the numbers of efferent connections to spiny neurons (see Results and Fig. 7). In future experiments it would be of interest to assess immunoreactivity to PV and the axonal arbors of these presumably immature interneurons. Of relevance to this possibility are our previous findings that anatomical abnormalities that indicate delayed maturation occur in calbindin-containing interneurons within the microgyrus proper (Kharazia *et al.*, 2003). Alterations in postsynaptic $GABA_A$ receptors such as decreased receptor density might also reduce postsynaptic conductance (Fig. 8B1) without a significant change in the kinetics of the evoked uIPSCs (Fig. 8B3,4).

Our results in spiny cells in layer IV of the PMG zone agree partly with those obtained previously from pyramidal cells in layer V of the epileptogenic area in the microgyrus model (Jacobs and Prince, 2005). In both studies, the conductance of sIPSCs increases whereas that of sEPSPs does not. However in layer V, the conductance of monosynaptic IPSCs was unchanged from control, in contrast to the significant reduction in uIPSCs in spiny cells of layer IV reported here. There is precedent for a differential reduction in IPSCs in layer IV compared to layer V pyramidal cells in epileptic *tottering* mice, presumably because of differences in presynaptic Ca^{2+} channels in terminals of FS cells (Sasaki *et al.*, 2006). It is also likely that other subtypes of interneurons contribute to sIPSCs and polysynaptic evoked IPSCs in both layers IV and V, perhaps accounting for the discrepancy between reduced conductance of uIPSCs from FS cells and the increase in sIPSC conductance in the current results. Other possible explanations include an increase in the contacts provided by one interneuron subtype and a decrease in those from another (Buckmaster and Dudek, 1997), and a reduction in overall interneuron number with compensatory sprouting and formation of inhibitory synapses by surviving interneurons (Nieoullon and Dusticier, 1981; Katsumaru *et al.*, 1986; Davenport *et al.*, 1990; Wittner *et al.*, 2001).

Another potential mechanism underlying epileptogenesis associated with microgyri is enhanced excitatory connectivity, as evidenced by the increased frequency of sEPSCs and mEPSCs in subgroups of layer V PMG cells and the marked reductions in sIPSC frequency induced by perfusion with glutamate-receptor blockers (Jacobs and Prince, 2005), as well as by increases in sEPSC frequency in the present study (Table 2). The increased density of axons in the immediate paramicrogyral area (Fig. 1B), enhanced glutamate immunoreactivity of axonal projections in this area (Humphreys *et al.*, 1991) and increased thalamocortical projections to areas of aberrantly structured barrels (Jacobs *et al.*, 1999c) all indicate restructuring of excitatory inputs. Whether this restructuring also affects recurrent connections of spiny cells in the PMG is not known. In both hippocampal slice cultures (McKinney *et al.*, 1997), and epileptogenic partially isolated cortex (Jin *et al.*, 2006), it appears that aberrant excitatory connectivity involves individual pyramidal cells making contacts on a wider field of targets, rather than more synapses on single postsynaptic cells, There was no significant increase in the amplitude of uEPSCs in the PMG, which indicates that enhanced connectivity between spiny cells, if present, involves more widespread projections rather than increased connectivity between cell pairs. In addition, the lateral spread of

Table 1. Properties of sIPSCs in spiny neurons in control and FL cortices.

	Peak amplitude (pA)	Half-width (ms)	Rise time (ms)	Decay time (ms)	Area (pA · ms)	Inst. frequency (Hz)	*n*
Control	10.2 ± 2.0	14.2 ± 2.1	3.2 ± 0.4	19.6 ± 3.6	238 ± 40	5.6 ± 1.2	12
FL area 0	6.9 ± 1.8*	13.0 ± 1.6	2.9 ± 0.3	15.4 ± 1.7	144 ± 17*	4.7 ± 1.3	8
FL area 1	14.7 ± 3.3*	12.8 ± 3.2	3.3 ± 0.6	21.7 ± 4.4	214 ± 105	7.2 ± 1.1*	12
FL area 2	18.3 ± 5.1*	16.6 ± 3.1	3.3 ± 0.4	21.5 ± 1.3	258 ± 88	4.7 ± 0.9	6

$P < 0.05$ compared to controls. FL area 0, within the microgyrus; FL area 1, area adjacent to (average 0.3 mm from) the border of the microgyrus; FL area 2, area far (∼1 mm) from the microgyrus.

Table 2. Properties of sEPSCs in spiny neurons of control and FL-treated cortices.

	Peak amplitude (pA)	Half-width (ms)	Rise time (ms)	Decay time (ms)	Area (pA · ms)	Inst. frequency (Hz)	*n*
Control	−11.8 ± 1.9	8.8 ± 1.0	3.3 ± 0.5	10.8 ± 1.1	−125 ± 17	9.4 ± 1.1	12
FL area 0	−8.1 ± 0.8	8.6 ± 0.9	2.7 ± 0.3	9.7 ± 1.0	−88 ± 12	8.1 ± 1.2	8
FL area 1	−12.8 ± 1.6	6.2 ± 1.3	4.3 ± 0.6	7.5 ± 1.3	−139 ± 26	15.6 ± 1.9*	12
FL area 2	−8.3 ± 1.1	9.2 ± 1.2	2.7 ± 0.3	8.5 ± 1.3	−96 ± 25	8.3 ± 1.4	6

*$P < 0.05$ compared to controls. FL area 0, within the microgyrus; FL area 1, area adjacent to (average 0.3 mm from) the border of the microgyrus; FL area 2, area further (~1 mm) from microgyrus.

epileptiform activity (Fig. 2B) might result from decreased GABAergic inhibition only (Prince and Wilder, 1967; Miles and Wong, 1987; Chagnac-Amitai and Connors, 1989).

GABAergic cells in the neocortex and hippocampus provide stability to the principal neuronal population by feed-back and feed-forward inhibition that prevents development and spread of epileptogenic discharges (Prince and Wilder, 1967; Wong and Prince, 1979; Chagnac-Amitai and Connors, 1989). A decrease in normally powerful thalamocortically-evoked GABAergic inhibition from FS interneurons in barrel cortex is likely to have important functional consequences because of the resulting prolonged excitation of spiny (excitatory) cells (Sun *et al.*, 2006). In addition, GABAergic neurons participate actively in cortical maturation in rodents, primates and humans (Owens *et al.*, 1999; Levitt *et al.*, 2004). Much cortical development occurs late in gestation and postnatally, making these high-risk periods when pathological processes can lead to developmental abnormalities and associated neuropsychiatric disorders (Marin and Rubenstein, 2001; Marin and Rubenstein, 2003). Defects in either the production or migration of cortical GABAergic neurons and GABA receptor abnormalities result in a hyper-excitable cortex, epilepsy and cognitive dysfunction (Hensch *et al.*, 1998; Harkin *et al.*, 2002; Powell *et al.*, 2003; Marini *et al.*, 2003). Apparent increases in cortical inhibition, described in other models of epilepsy (Buhl *et al.*, 1996; Klaassen *et al.*, 2006) are likely to be caused by GABAergic synchronization of excitatory cortical activity necessary to initiate the spread of epileptiform activity (Troyer *et al.*, 1992; Michelson and Wong, 1994; Engel, 1995; Kohling *et al.*, 2000; Avoli *et al.*, 2002; Khazipov and Holmes, 2003).

In the neonatal freeze-lesion model, the most epileptogenic zone is the cortical region immediately adjacent to the microgyrus (Jacobs *et al.*, 1996; Jacobs *et al.*, 1999a; Jacobs *et al.*, 1999c). This paramicrogyral zone has grossly normal cytoarchitectonic organization, however alterations in postsynaptic receptors and synaptic strength are present (DeFazio and Hablitz, 1999; DeFazio and Hablitz, 2000; Jacobs and Prince, 2005) as well as abnormal connectivity (Jacobs *et al.*, 1999c; Rosen *et al.*, 2000) and widespread reductions in the density of PV-containing GABAergic interneurons (Rosen *et al.*, 1998; but see Schwarz *et al.*, 2000). Apparent loss of inhibitory neurons or decreases in functional inhibition is also reported in cortical dysplasia produced by fetal irradiation (Roper *et al.*, 1997; Roper, 1998; Zhu and Roper, 2000; Chen and Roper, 2003) and in human dysplastic cortex (Calcagmoto *et al.*, 2005), and is a common finding in other models of chronic epileptogenesis (Ribak *et al.*, 1986; Lowenstein *et al.*, 1992; Buckmaster and Dudek, 1997; Cossart *et al.*, 2001; reviewed in Prince and Jacobs, 1998).

Our results show that the strength of unitary inhibitory responses from FS cells onto spiny cells is affected severely in barrels in the PMG region whereas excitatory connections between two spiny cells within a barrel circuit are not changed. The selective downregulation of basket cell output might be sufficient to induce epileptiform activities in neocortex. Results indicate that thalamically evoked cortical responses are regulated predominantly by basket cells whose output is a key factor controlling excitability in the thalamocortical circuit. Disorders in either these neurons or their functional connections leads to the generation and propagation of epileptiform discharges.

ACKNOWLEDGEMENTS

We thank Isabel Parada for expert histological support. This work was supported by Grants 06477 and 12151 from the NINDS.

REFERENCES

Agmon A. and Connors B.W. (1991) Thalamocortical responses of mouse somatosensory (barrel) cortex in vitro. *Neuroscience* 41, 365–379.

Agmon A. and Connors B.W. (1992) Correlation between intrinsic firing patterns and thalamocortical synaptic responses of neurons in mouse barrel cortex. *Journal of Neuroscience* 12, 319–329.

Agmon A., Yang L.T., Jones E.G. and O'Dowd D.K. (1995) Topological precision in the thalamic projection to neonatal mouse barrel cortex. *Journal of Neuroscience* 15, 549–561.

Alonso-Nanclares L., Garbelli R., Sola R.G., Pastor J., Tassi L., Spreafico R. *et al.* (2005) Microanatomy of the dysplastic neocortex from epileptic patients. *Brain* 128, 158–173.

Avoli M., D'Antuono M., Louvel J., Kohling R., Biagini G., Pumain R. *et al.* (2002) Network and pharmacological mechanisms leading to epileptiform synchronization in the limbic system in vitro. *Progress in Neurobiology* 68, 167–207.

Beierlein M., Gibson J.R. and Connors B.W. (2000) A network of electrically coupled interneurons drives synchronized inhibition in neocortex. *Nature Neuroscience* 3, 904–910.

Brecht M. and Sakmann B. (2002) Whisker maps of neuronal subclasses of the rat ventral posterior medial thalamus, identified by whole-cell voltage recording and morphological reconstruction. *Journal of Physiology* 538, 495–515.

Buckmaster P.S. and Dudek F.E. (1997) Network properties of the dentate gyrus in epileptic rats with hilar neuron loss and granule cell axon reorganization. *Journal of Neurophysiology* 77, 2685–2696.

Buhl E.H., Otis T.S. and Mody I. (1996) Zinc-induced collapse of augmented inhibition by GABA in a temporal lobe epilepsy model. *Science* 271, 369–373.

Calcagnotto M.E., Paredes M.F., Tiban T., Barbaro N.M. and Baraban S.C. (2005) Dysfunction of synaptic inhibition in epilepsy associated with focal cortical dysplasia. *Journal of Neuroscience* 25, 9649–9657.

Chagnac-Amitai Y. and Connors B.W. (1989) Horizontal spread of synchronized activity in neocortex and its control by GABA-mediated inhibition. *Journal of Neurophysiology* 61, 747–758.

Chen H.X. and Roper S.N. (2003) Reduction of spontaneous inhibitory activity in experimental heterotopic gray matter. *Journal of Neurophysiology* 89, 150–158.

Chevassus-Au-Louis N., Baraban S.C., Gaiarsa J.L. and Ben Ari Y. (1999a) Cortical malformations and epilepsy: new insights from animal models. *Epilepsia* 40, 811–821.

Chevassus-Au-Louis N., Jorquera I., Ben Ari, Y. and Represa A. (1999b) Abnormal connections in the malformed cortex of rats with prenatal treatment with methylazoxymethanol may support hyperexcitability. *Developmental Neuroscience* 21, 385–392.

Chevassus-Au-Louis N. and Represa A. (1999) The right neuron at the wrong place: biology of heterotopic neurons in cortical neuronal migration disorders, with special reference to associated pathologies. *Cellular and Molecular Life Sciences: CMLS* 55, 1206–1215.

Cossart R., Dinocourt C., Hirsch J.C., Merchan-Perez A., De Felipe J., Esclapez M. *et al.* (2001) Dendritic but not somatic GABAergic inhibition is decreased in experimental epilepsy. *Nature Neuroscience* 4, 52–62.

Davenport C.J., Brown W.J. and Babb T.L. (1990) Sprouting of GABAergic and mossy fiber axons in dentate gyrus following intrahippocampal kainate in the rat. *Experimental Neurology* 109, 180–190.

DeFazio R.A. and Hablitz J.J. (1999) Reduction of zolpidem sensitivity in a freeze lesion model of neocortical dysgenesis. *Journal of Neurophysiology* 81, 404–407.

DeFazio R.A. and Hablitz J.J. (2000) Alterations in NMDA receptors in a rat model of cortical dysplasia. *Journal of Neurophysiology* 83, 315–321.

Dvorák K. and Feit J. (1977) Migration of neuroblasts through partial necrosis of the cerebral cortex in newborn rats—Contribution to the problems of morphological development and developmental period of cerebral microgyria. *Acta Neuropathol. (Berl.)* 38, 203–212.

Dvorák K., Feit J. and Juránková Z. (1978) Experimentally induced focal microgyria and status verrucosus deformis in rats—Pathogenesis and interrelation histological and autoradiographical study. *Acta Neuropathologica* 44, 121–129.

Engel J., Jr (1995) Inhibitory mechanisms of epileptic seizure generation. *Advances in Neurology* 67, 157–171.

Evrard P. (1988) Disorders in the prenatal development of the human cortex. *Bulletin et Mémoires de l'Académie Royale de Médecine de Belgique* 143, 356–368.

Evrard P. (1997) Genetic and environmental determinants of neocortical development. *Pediatric Pulmonology. Supplement* 16, 213–215.

Feldmeyer D., Egger V., Lubke J. and Sakmann B. (1999) Reliable synaptic connections between pairs of excitatory layer 4 neurones within a single 'barrel' of developing rat somatosensory cortex. *Journal of Physiology* 521 Pt 1, 169–190.

Feldmeyer D., Lubke J., Silver R.A. and Sakmann B. (2002) Synaptic connections between layer 4 spiny neurone-layer 2/3 pyramidal cell pairs in juvenile rat barrel cortex: physiology and anatomy of interlaminar signalling within a cortical column. *Journal of Physiology* 538, 803–822.

Gibson J.R., Beierlein M.and Connors B.W. (1999) Two networks of electrically coupled inhibitory neurons in neocortex. *Nature* 402, 75–79.

Gupta A., Wang Y. and Markram H. (2000) Organizing principles for a diversity of GABAergic interneurons and synapses in the neocortex. *Science* 287, 273–278.

Hagemann G., Kluska M.M., Redecker C., Luhmann H.J. and Witte O.W. (2003) Distribution of glutamate receptor subunits in experimentally induced cortical malformations. *Neuroscience* 117, 991–1002.

Harkin L.A., Bowser D.N., Dibbens L.M., Singh R., Phillips F., Wallace R.H. *et al.* (2002) Truncation of the GABA(A)-receptor gamma2 subunit in a family with generalized epilepsy with febrile seizures plus. *American Journal of Human Genetics* 70, 530–536.

Hensch T.K., Fagiolini M., Mataga N., Stryker M.P., Baekkeskov S. and Kash S.F. (1998) Local GABA circuit control of experience-dependent plasticity in developing visual cortex. *Science* 282, 1504–1508.

Humphreys P., Rosen G.D., Press D.M., Sherman G.F. and Galaburda A.M. (1991) Freezing lesions of the developing rat brain: a model for cerebrocortical microgyria. *Journal of Neuropathology and Experimental Neurology* 50, 145–160.

Inoue T. and Imoto K. (2006) Feedforward inhibitory connections from multiple thalamic cells to multiple regular-spiking cells in layer 4 of the somatosensory cortex. *Journal of Neurophysiology* 96, 1746–1754.

Jacobs K.M., Gutnick M.J. and Prince D.A. (1996) Hyperexcitability in a model of cortical maldevelopment. *Cerebral Cortex* 6, 514–523.

Jacobs K.M., Hwang B.J. and Prince D.A. (1999a) Focal epileptogenesis in a rat model of polymicrogyria. *Journal of Neurophysiology* 81, 159–173.

Jacobs K.M., Kharazia V.N. and Prince D.A. (1999b) Mechanisms underlying epileptogenesis in cortical malformations. *Epilepsy Research* 36, 165–188.

Jacobs K.M., Mogensen M., Warren E. and Prince D.A. (1999c) Experimental microgyri disrupt the barrel field pattern in rat somatosensory cortex. *Cerebral Cortex* 9, 733–744.

Jacobs K.M. and Prince D.A. (2005) Excitatory and inhibitory postsynaptic currents in a rat model of epileptogenic microgyria. *Journal of Neurophysiology* 93, 687–696.

Jin X., Prince D.A. and Huguenard J.R. (2006) Enhanced excitatory synaptic connectivity in layer v pyramidal neurons of chronically injured epileptogenic neocortex in rats. *Journal of Neuroscience* 26, 4891–4900.

Katsumaru H., Murakami F., Wu J.Y. and Tsukahara N. (1986) Sprouting of GABAergic synapses in the red nucleus after lesions of the nucleus interpositus in the cat. *Journal of Neuroscience* 6, 2864–2874.

Keller A. and White E.L. (1987) Synaptic organization of GABAergic neurons in the mouse SmI cortex. *Journal of Comparative Neurology* 262, 1–12.

Kharazia V.N., Jacobs K.M. and Prince D.A. (2003) Light microscopic study of GluR1 and calbindin expression in interneurons of neocortical microgyral malformations. *Neuroscience* 120, 207–218.

Khazipov R. and Holmes G.L. (2003) Synchronization of kainate-induced epileptic activity via GABAergic inhibition in the superfused rat hippocampus in vivo. *Journal of Neuroscience* 23, 5337–5341.

Kim H.G., Fox K. and Connors B.W. (1995) Properties of excitatory synaptic events in neurons of primary somatosensory cortex of neonatal rats. *Cerebral Cortex* 5, 148–157.

Klaassen A., Glykys J., Maguire J., Labarca C., Mody I. and Boulter J. (2006) Seizures and enhanced cortical GABAergic inhibition in two mouse models of human autosomal dominant nocturnal frontal lobe epilepsy. *Proceedings of the National Academy of Sciences of the USA* 103, 19152–19157.

Kohling R., Vreugdenhil M., Bracci E. and Jefferys J.G. (2000) Ictal epileptiform activity is facilitated by hippocampal GABAA receptor-mediated oscillations. *Journal of Neuroscience* 20, 6820–6829.

Lee K., Schottler F., Collins J., Lanzino G., Couture D., Rao A. *et al.* (1997) A genetic animal model of human neocortical heterotopia associated with seizures. *Journal of Neuroscience* 17, 6236–6242.

Levitt P., Eagleson K.L. and Powell E.M. (2004) Regulation of neocortical interneuron development and the implications for neurodevelopmental disorders. *Trends in Neurosciences* 27, 400–406.

Lowenstein D.H., Thomas M.J., Smith D.H. and McIntosh T.K. (1992) Selective vulnerability of dentate hilar neurons following traumatic brain injury: a potential mechanistic link between head trauma and disorders of the hippocampus. *Journal of Neuroscience* 12, 4846–4853.

McCormick D.A., Connors B.W., Lighthall J.W. and Prince D.A. (1985) Comparative electrophysiology of pyramidal and sparsely spiny stellate neurons of the neocortex. *Journal of Neurophysiology* 54, 782–806.

McKinney R.A., Debanne D., Gahwiler B.H. and Thompson S.M. (1997) Lesion-induced axonal sprouting and hyperexcitability in the hippocampus in vitro: implications for the genesis of posttraumatic epilepsy. *Nature Medicine* 3, 990–996.

Marin O. and Rubenstein J.L. (2001) A long, remarkable journey: tangential migration in the telencephalon. *Nature Reviews Neuroscience* 2, 780–790.

Marin O. and Rubenstein J.L. (2003) Cell migration in the forebrain. *Annual Review of Neuroscience* 26, 441–483.

Marini C., Harkin L.A., Wallace R.H., Mulley J.C., Scheffer I.E. and Berkovic S.F. (2003) Childhood absence epilepsy and febrile seizures: a family with a GABA(A) receptor mutation. *Brain* 126, 230–240.

Matsumoto H. and Ajmone-Marsan C. (1964) Cortical cellular phenomena in experimental epilepsy: interictal manifestations. *Experimental Neurology* 9, 286–304.

Michelson H.B. and Wong R.K. (1994) Synchronization of inhibitory neurones in the guinea-pig hippocampus in vitro. *Journal of Physiology (Lond.)* 477, 35–45.

Miles R. and Wong R.K. (1987) Latent synaptic pathways revealed after tetanic stimulation in the hippocampus. *Nature* 329, 724–726.

Nieoullon A. and Dusticier N. (1981) Increased glutamate decarboxylase activity in the red nucleus of the adult cat after cerebellar lesions. *Brain Research* 224, 129–139.

Owens D.F., Liu X. and Kriegstein A.R. (1999) Changing properties of GABA(A) receptor-mediated signaling during early neocortical development. *Journal of Neurophysiology* 82, 570–583.

Porter J.T., Johnson C.K. and Agmon A. (2001) Diverse types of interneurons generate thalamus-evoked feedforward inhibition in the mouse barrel cortex. *Journal of Neuroscience* 21, 2699–2710.

Powell E.M., Campbell D.B., Stanwood G.D., Davis C., Noebels J.L. and Levitt P. (2003) Genetic disruption of cortical interneuron development causes region- and GABA cell type-specific deficits, epilepsy, and behavioral dysfunction. *Journal of Neuroscience* 23, 622–631.

Prince D.A. (1968) The depolarization shift in "epileptic" neurons. *Experimental Neurology* 21, 467–485.

Prince D.A. and Jacobs K.M. (1998) Inhibitory function in two models of chronic epileptogenesis. *Epilepsy Research* 32, 82–92.

Prince D.A. and Wilder B.J. (1967) Control mechanisms in cortical epileptogenic foci. "Surround" inhibition. *Archives of Neurology* 16, 194–202

Raymond A.A., Fish D.R., Boyd S.G., Smith S.J., Pitt M.C. and Kendall B. (1995) Cortical dysgenesis: serial EEG findings in children and adults. *Electroencephalography and Clinical Neurophysiology* 94, 389–397.

Ribak C.E., Hunt C.A., Bakay R.A. and Oertel W.H. (1986) A decrease in the number of GABAergic somata is associated with the preferential loss of GABAergic terminals at epileptic foci. *Brain Research* 363, 78–90.

Roper S.N. (1998) In utero irradiation of rats as a model of human cerebrocortical dysgenesis: a review. *Epilepsy Research* 32, 63–74.

Roper S.N., King M.A., Abraham L.A. and Boillot M.A. (1997) Disinhibited in vitro neocortical slices containing experimentally induced cortical dysplasia demonstrate hyperexcitability. *Epilepsy Research* 26, 443–449.

Rosen G.D., Burstein D. and Galaburda A.M. (2000) Changes in efferent and afferent connectivity in rats with induced cerebrocortical microgyria. *Journal of Comparative Neurology* 418, 423–440.

Rosen G.D., Jacobs K.M. and Prince D.A. (1998) Effects of neonatal freeze lesions on expression of parvalbumin in rat neocortex. *Cerebral Cortex* 8, 753–761.

Sasaki S., Huda K., Inoue T., Miyata M. and Imoto K. (2006) Impaired feedforward inhibition of the thalamocortical projection in epileptic Ca2+ channel mutant mice, tottering. *Journal of Neuroscience* 26, 3056–3065.

Schwarz P., Stichel C.C. and Luhmann H.J. (2000) Characterization of neuronal migration disorders in neocortical structures: loss or preservation of inhibitory interneurons? *Epilepsia* 41, 781–787

Schwartzkroin P.A. and Walsh C.A. (2000) Cortical malformations and epilepsy. *Mental Retardation and Developmental Disabilities Research Reviews* 6, 268–280.

Sillito A.M. (1977) Inhibitory processes underlying the directional specificity of simple, complex and hypercomplex cells in the cat's visual cortex. *Journal of Physiology* 271, 699–720.

Simons D.J. (1978) Response properties of vibrissa units in rat SI somatosensory neocortex. *Journal of Neurophysiology* 41, 798–820.

Simons D.J. and Woolsey T.A. (1979) Functional organization in mouse barrel cortex. *Brain Research* 165, 327–332.

Spreafico R., Battaglia G., Arcelli P., Andermann F., Dubeau F., Palmini A. *et al.* (1998) Cortical dysplasia: an immunocytochemical study of three patients. *Neurology* 50, 27–36.

Sun Q.Q., Huguenard J.R. and Prince D.A. (2006) Barrel cortex microcircuits: thalamocortical feedforward inhibition in spiny stellate cells is mediated by a small number of fast-spiking interneurons. *Journal of Neuroscience* 26, 1219–1230.

Troyer M.D., Blanton M.G. and Kriegstein A.R. (1992) Abnormal action-potential bursts and synchronized, gaba-mediated inhibitory potentials in an in vitro model of focal epilepsy. *Epilepsia* 33, 199–212.

Wang Y., Gupta A., Toledo-Rodriguez M., Wu C.Z. and Markram H. (2002) Anatomical, physiological, molecular and circuit properties of nest basket cells in the developing somatosensory cortex. *Cerebral Cortex* 12, 395–410.

Weinberger D.R. and Lipska B.K. (1995) Cortical maldevelopment, antipsychotic drugs, and schizophrenia: a search for common ground. *Schizophrenia Research* 16, 87–110.

Wittner L., Magloczky Z., Borhegyi Z., Halasz P., Toth S., Eross L. *et al.* (2001) Preservation of perisomatic inhibitory input of granule cells in the epileptic human dentate gyrus. *Neuroscience* 108, 587–600.

Wong R.K. and Prince D.A. (1979) Dendritic mechanisms underlying penicillin-induced epileptiform activity. *Science* 204, 1228–1231.

Wong-Riley M. (1979) Changes in the visual system of monocularly sutured or enucleated cats demonstrable with cytochrome oxidase histochemistry. *Brain Research* 171, 11–28.

Woolsey T.A. (1967) Somatosensory, auditory and visual cortical areas of the mouse. *Johns Hopkins Medical Journal* 121, 91–112.

Woolsey T.A. and Van der Loos H. (1970) The structural organization of layer IV in the somatosensory region (SI) of mouse cerebral cortex. The description of a cortical field composed of discrete cytoarchitectonic units. *Brain Research* 17, 205–242.

Zhu W.J. and Roper S.N. (2000) Reduced inhibition in an animal model of cortical dysplasia. *Journal of Neuroscience* 20, 8925–8931.

Zilles K., Qu M., Schleicher A. and Luhmann H.J. (1998) Characterization of neuronal migration disorders in neocortical structures: quantitative receptor autoradiography of ionotropic glutamate, GABA(A) and GABA(B) receptors. *European Journal of Neuroscience* 10, 3095–3106.

Correspondence should be addressed to:
J.R. Huguenard
Dept of Neurology and Neurological Sciences
Stanford University
Stanford CA 94301, USA
email: John.Huguenard@Stanford.Edu